iScience

CellPress
OPEN ACCESS

Article

The NF-κB/NUAK2 signaling axis regulates pancreatic cancer progression by targeting SMAD2/3

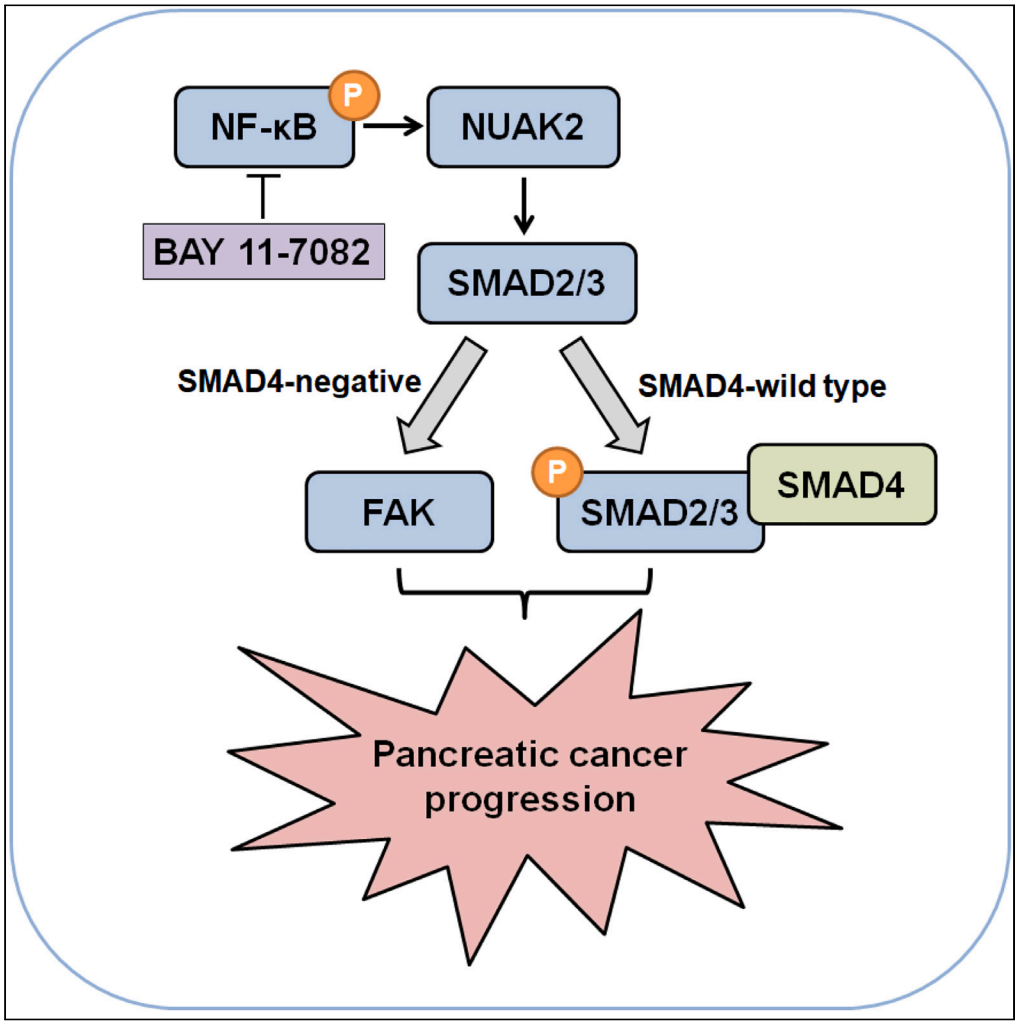

Ruobing Wang, Dan Su, Yueze Liu, ..., Jinxin Tao, Guihu Weng, Taiping Zhang

tpingzhang@yahoo.com

Highlights

NUAK2 silencing hampers the progression of pancreatic cancer

NUAK2 is transcriptionally regulated by NF-κB in pancreatic cancer

NUAK2 mediates oncogenic effects in pancreatic cancer by targeting SMAD2/3

NUAK2 silencing increases the sensitivity of pancreatic cancer cells to gemcitabine

Wang et al., iScience 27, 109406
April 19, 2024
https://doi.org/10.1016/j.isci.2024.109406

iScience

CellPress
OPEN ACCESS

Article

The NF-κB/NUAK2 signaling axis regulates pancreatic cancer progression by targeting SMAD2/3

Ruobing Wang,[1,3] Dan Su,[1,3] Yueze Liu,[1] Hua Huang,[1] Jiangdong Qiu,[1] Zhe Cao,[1] Gang Yang,[1] Hao Chen,[1] Wenhao Luo,[1] Jinxin Tao,[1] Guihu Weng,[1] and Taiping Zhang[1,2,4,*]

SUMMARY

Nuclear factor kappa B (NF-κB) plays a pivotal role in the development of pancreatic cancer, and its phosphorylation has previously been linked to the regulation of NUAK2. However, the regulatory connection between NF-κB and NUAK2, as well as NUAK2's role in pancreatic cancer, remains unclear. In this study, we observed that inhibiting NUAK2 impeded the proliferation, migration, and invasion of pancreatic cancer cells while triggering apoptosis. NUAK2 overexpression partially resisted apoptosis and reversed the inhibitory effects of the NF-κB inhibitor. NF-κB transcriptionally regulated NUAK2 transcription by binding to the promoter region of NUAK2. Mechanistically, NUAK2 knockdown remarkably reduced the expression levels of *p*-SMAD2/3 and SMAD2/3, resulting in decreased nuclear translocation of SMAD4. In SMAD4-negative cells, NUAK2 knockdown impacted FAK signaling by downregulating SMAD2/3. Moreover, NUAK2 knockdown heightened the sensitivity of pancreatic cancer cells to gemcitabine, suggesting that NUAK2 inhibitors could be a promising strategy for pancreatic cancer treatment.

INTRODUCTION

Pancreatic cancer is one of the most malignant forms of cancer, with a 5-year survival rate as low as 12%.[1,2] Due to its subtle onset and heightened malignancy, the disease often remains undetected until it reaches an advanced stage. While surgical resection offers potential as a curative measure, only 15–20% of patients with early-stage tumors are eligible for such intervention.[3] Current pancreatic cancer management employs various treatments, such as chemotherapy, radiotherapy, immunotherapy, and targeted therapy.[4] However, patients' prognoses following these treatments showed limited improvement, probably due to the challenging aspects of high recurrence and metastasis rates. Consequently, further studies are needed to explore novel mechanisms underlying pancreatic cancer, thereby offering new therapeutic strategies and better drug options for improving the prognosis of pancreatic cancer.

The nuclear factor kappa B (NF-κB) family comprises transcription factors, such as RelA (p65), RelB, c-Rel, NF-κB1 (p105-p50), and NF-κB2 (p100-p52), ubiquitously present in cells.[5,6] Inhibitors of NF-κB (IκB) can impede the nuclear transport process of NF-κB transcription factors, maintaining them in an inactive state in the cytoplasm.[7] NF-κB plays a crucial role in cellular stress and inflammation, and its activation is also observed in various cancers, establishing it as a key signaling mediator in the occurrence and progression of numerous malignancies.[8–11] Notably, NF-κB activation has been reported in pancreatic cancer, a disease characterized by high inflammation, suggesting its involvement in both cancer and cancer-related inflammation.[12] NF-κB plays a role in the proliferation, invasion, metastasis, and angiogenesis of pancreatic cancer and contributes to drug resistance by regulating resistance-related proteins, underscoring its critical role in pancreatic cancer.[13–19]

The Novel (nua) kinase family 2 (NUAK2), also known as SNARK, is one of the prominent members of adenosine monophosphate-activated protein kinase (AMPK)-related kinases and is widely expressed across various human tissues.[20] These kinases play important roles in cell metabolism and motility.[21,22] The regulation of NUAK2 is also linked to human diseases like obesity and cancer.[20,23] The analysis of The Cancer Genome Atlas (TCGA) database revealed frequent amplification of NUAK2 in human cancers, especially breast and liver cancer.[24] While recent studies have underscored the essential roles of NUAK2 in several cancers, its specific function in pancreatic cancer remains undefined. Concurrently, reports indicate that the up-regulation of NUAK2 in response to stress depends on the activation of NF-κB. NUAK2 overexpression enhances tumor cells' resistance to CD95-mediated apoptosis.[25] Given the regulatory effect of NF-κB on NUAK2, we speculated that the NF-κB/NUAK2 axis plays a pivotal role in the development of pancreatic cancer.

This study aims to investigate the role of NUAK2 in pancreatic cancer and explore the regulatory relationship between NF-κB and NUAK2. Additionally, we examine the molecular mechanisms underlying the action of NUAK2 in pancreatic cancer.

[1]Department of General Surgery, Peking Union Medical College Hospital, Chinese Academy of Medical Sciences and Peking Union Medical College, Beijing 100730, China
[2]Clinical Immunology Center, Chinese Academy of Medical Sciences and Peking Union Medical College, Beijing 100730, China
[3]These authors contributed equally
[4]Lead contact
*Correspondence: tpingzhang@yahoo.com
https://doi.org/10.1016/j.isci.2024.109406

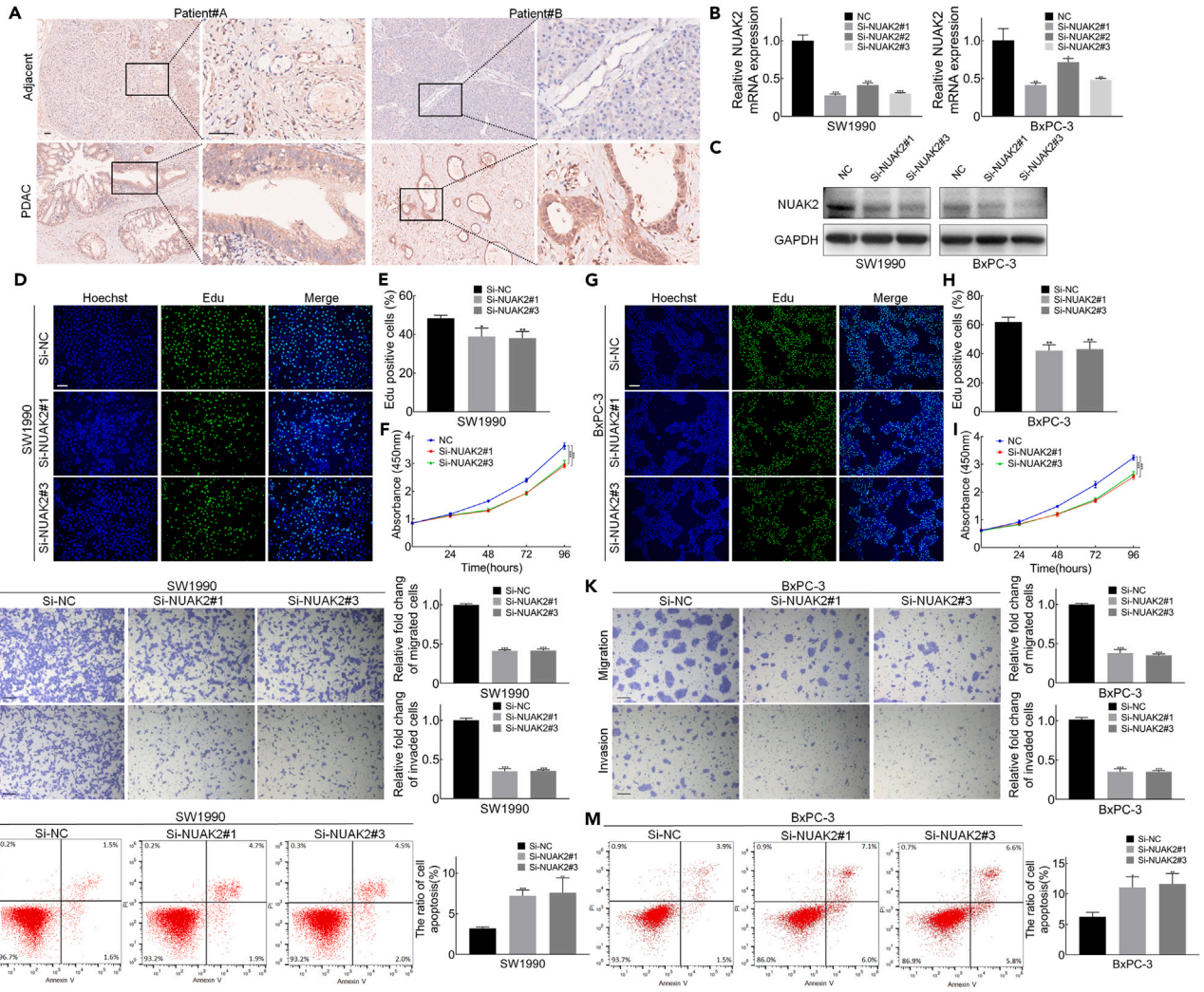

Figure 1. NUAK2 silencing inhibited the proliferation, migration, and invasion of pancreatic cancer cells and induced cell apoptosis

(A) Representative IHC images showing intensive NUAK2 staining in surgically resected PDAC samples, but weak in the adjacent non-cancerous tissues from patients. Scale bar: 50 μm.

(B) The expression of NUAK2 mRNA was assessed by qRT-PCR in SW1990 and BxPC-3 cells treated with Si-NUAK2 or Si-NC for 48h. The gene was normalized to GAPDH.

(C) Western blot analysis was performed with NUAK2 and GAPDH antibodies. GAPDH was used as the loading control.

(D–I) SW1990 and BxPC-3 cells were transfected with Si-NUAK2 or Si-NC. EdU assays showing that knockdown of NUAK2 inhibited the DNA synthesis of pancreatic cancer cells. The viability of cells was determined by CCK-8 assay. Scale bar: 100 μm.

(J and K) The cell migration and invasion ability were measured using transwell migration and Matrigel invasion assays after knocking down NUAK2 in SW1990 and BxPC-3 cells. Scale bar: 100 μm.

(L and M) Apoptosis was analyzed by flow cytometry stained with Annexin V/PI after transfected with Si-NUAK2 or Si-NC for 48h. Data are presented as the mean ± SEM, *p < 0.05, **p < 0.01, ***p < 0.001. Statistical analysis was performed using Student's *t* test.

RESULTS

NUAK2 silencing inhibited the proliferation, migration, and invasion of pancreatic cancer cells and induced cell apoptosis

Previous studies have consistently indicated frequent amplification of NUAK2 in various human cancers.[24] To investigate the expression of NUAK2 in pancreatic cancer, we conducted immunohistochemical (IHC) staining of NUAK2 in pancreatic ductal adenocarcinoma (PDAC) and adjacent non-cancerous tissues. Our findings revealed that NUAK2 was highly expressed in PDAC tissues compared to adjacent non-cancerous tissues (Figure 1A).

To further evaluate the role of NUAK2 in pancreatic cancer cells, we employed short interfering RNAs (siRNA) transfection to knock down NUAK2 in SW1990 and BxPC-3 cells. The efficiency of Si-NUAK2 transfection in pancreatic cancer cells was validated through qRT-PCR and

western blotting (Figures 1B and 1C). Si-NUAK2#1 and Si-NUAK2#3 were selected for subsequent experiments. EdU and CCK-8 assays demonstrated that the knockdown of NUAK2 suppressed the proliferation of pancreatic cancer cells (Figures 1D–1I). Additionally, we explored the impact of NUAK2 silencing on the migration and invasion capabilities of pancreatic cancer cells. The results showed a noticeable reduction in the migration and invasion abilities of SW1990 and BxPC-3 cells upon NUAK2 knockdown, as evidenced by transwell assays (Figures 1J and 1K). Further analysis using flow cytometry revealed that Si-NUAK2 facilitated the apoptosis of pancreatic cancer cells (Figures 1L and 1M). Taken together, these findings suggested that NUAK2 knockdown induced apoptosis while concurrently inhibiting the proliferation, migration, and invasion of pancreatic cancer cells *in vitro*.

Antitumor effect of NF-κB inhibitor in pancreatic cancer cells

BAY11-7082, identified as an NF-κB inhibitor known for diminishing p65 phosphorylation, has been widely used in several studies.[26–28] To explore the effect of NF-κB inhibitor on the viability of pancreatic cancer cells, SW1990 and BxPC-3 cells were subjected to varying concentrations of BAY11-7082 for 24 h and 48 h. CCK-8 assay results showed that BAY11-7082 exerted a dose- and time-dependent inhibition on the viability of pancreatic cancer cells (Figures 2A and 2B).

Employing transwell migration assays, we observed a significant reduction in the migratory capability of pancreatic cancer cells treated with BAY11-7082 (Figures 2C–2F). Flow cytometry further indicated an increase in apoptosis with escalating concentrations of BAY11-7082 in pancreatic cancer cells (Figures 2G–2J). To determine the changes in pancreatic cancer cells following 24 h of BAY11-7082 treatment, we assessed the expression of N-cadherin, E-cadherin, p-p65, p65, and NUAK2 using western blotting. The results demonstrated that BAY11-7082 inhibited N-cadherin, p-p65, and NUAK2 expression in SW1990 and BxPC-3 cells (Figures 2K and 2L), suggesting a potential regulation of NUAK2 by NF-κB activation in pancreatic cancer cells. Additionally, we investigated the mRNA and protein levels of NUAK2 after the p65 knockdown, confirming that the p65 knockdown led to a reduction in mRNA and protein expression of NUAK2 in pancreatic cells (Figure S1).

NUAK2 overexpression partially reversed the anti-tumor effect of NF-κB inhibitor in pancreatic cancer cells

To elucidate the regulatory effect of NF-κB on NUAK2 expression in pancreatic cancer cells, we overexpressed NUAK2 in PANC-1 and AsPC-1 cells. Both mRNA and protein expression levels of NUAK2 significantly increased in transfected cells (Figures 3A and 3B). CCK-8 assays were conducted to assess the effect of NUAK2 overexpression on cell survival. The results revealed that the restoration of NUAK2 expression reversed the effect of BAY11-7082 on cell survival (Figures 3C and 3D). Flow cytometry showed that cells overexpressing NUAK2 displayed partial resistance to the apoptosis induced by the NF-κB inhibitor (Figures 3E–3H). Likewise, transwell assays indicated that the restoration of NUAK2 expression reversed the inhibitory effect of BAY11-7082 on cell migration (Figures 3I–3L). Western blot analysis further demonstrated that NUAK2 overexpression partially restored the downregulation of N-cadherin expression induced by BAY11-7082, while it had no noticeable effect on the expression of E-cadherin, p-p65, and p65 (Figures 3M and 3N). These cumulative results collectively suggested that NUAK2 overexpression partially reversed the inhibitory effects of NF-κB inhibitor on pancreatic cancer cells.

To further investigate whether NUAK2 kinase activity is crucial for restoring the antitumor effects of BAY11-7082, we constructed mutated NUAK2 (NUAK2-MUT) overexpression plasmid based on previously described methods.[29] CCK-8 assays were conducted to assess the effect of NUAK2-MUT overexpression on tumor survival. Interestingly, the restoration of NUAK2-MUT expression did not reverse the effects of BAY11-7082 on the survival of PANC-1 and AsPC-1 cells (Figures S2A and S2B). Flow cytometry indicated that cells overexpressing NUAK2-MUT were not resistant to NF-κB inhibitor-induced apoptosis (Figures S2C–S2F). Similarly, transwell assays demonstrated that the restoration of NUAK2-MUT expression did not reverse the effects of BAY11-7082 on cell migration (Figures S2G–S2J). Additionally, comparable amounts of NUAK2 protein were detected by western blotting in NUAK2-MUT and NUAK2 overexpressing cells (Figures S2K and S2L). Collectively, these results suggested that restoring the antitumor effects of NF-κB inhibitors depended on NUAK2 kinase activity.

NUAK2 was transcriptionally regulated by NF-κB

Given that the NF-κB pathway typically facilitates the transcription of target genes through nuclear translocations, we hypothesize that NF-κB may serve as a transcription factor promoting NUAK2 transcription. Two potential binding sites of p65 to the NUAK2 promoter region were identified using the JASPAR database (Figures 4A and 4B). To validate whether p65 directly binds to these potential sites in the NUAK2 promoter, a ChIP-quantitative real-time PCR (ChIP-qPCR) was performed. The results revealed a significant enrichment of p65 binding elements immunoprecipitated with the p65 antibody in the NUAK2 promoter, compared to those immunoprecipitated with the control antibody (Figures 4C and 4D). To determine the binding site of p65 to the NUAK2 promoter, we constructed luciferase reporter plasmids with the mutant promoter of NUAK2 (Mut1 and Mut2) (Figure 4E). Dual luciferase assays showed that the activities of NUAK2 wild-type (WT) and Mut2 promoters significantly increased when p65 was overexpressed. However, the activity of the NUAK2 Mut1 promoter showed no significant change with overexpression of p65 (Figures 4F and 4G). These findings confirmed that NF-κB promoted the transcription of NUAK2 by binding to the promoter region of NUAK2.

NUAK2 mediated oncogenic effects in pancreatic cancer by targeting SMAD2/3

Recent studies have indicated an association between NUAK2 and the transforming growth factor β (TGF-β) signaling pathway.[30,31] TGF-β signaling pathways play a crucial role in determining cell differentiation, proliferation arrest, migration, and apoptosis.[32–34] Notably, TGF-β is implicated in pancreatic cancer tumorigenesis, particularly via the activation of SMAD pathways. Utilizing qRT-PCR, we explored potential

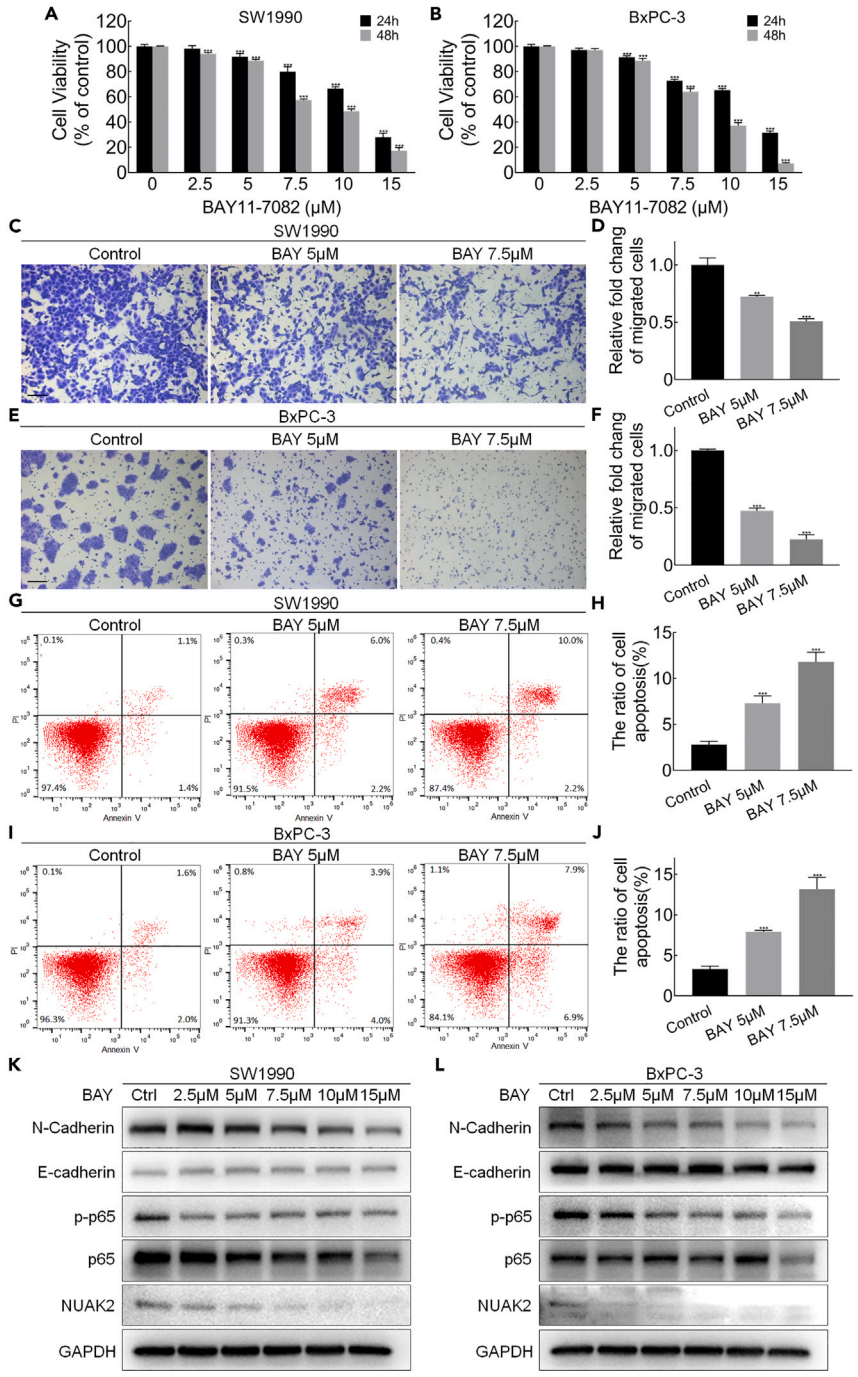

Figure 2. Antitumor effect of NF-κB inhibitor in pancreatic cancer cells

(A and B) SW1990 and BxPC-3 cells were treated with increasing concentrations of BAY11-7082 for 24h and 48h. The viability of cells was determined by CCK-8 assay.

(C–F) The cell migration ability was measured using transwell assays treated with BAY11-7082 for 20h. Scale bar: 100 μm.

(G–J) Apoptosis was analyzed by flow cytometry stained with Annexin V/PI after treated with BAY11-7082 for 18h.

(K and L) The expression of N-cadherin, E-cadherin, p-p65, p65, NUAK2 was examined in SW1990 and BxPC-3 cells treated with various concentrations of BAY11-7082 for 24h by using western blotting analysis. GAPDH was used as loading control. Data are presented as the mean ± SEM, *p < 0.05, **p < 0.01, ***p < 0.001. Statistical analysis was performed using Student's *t* test.

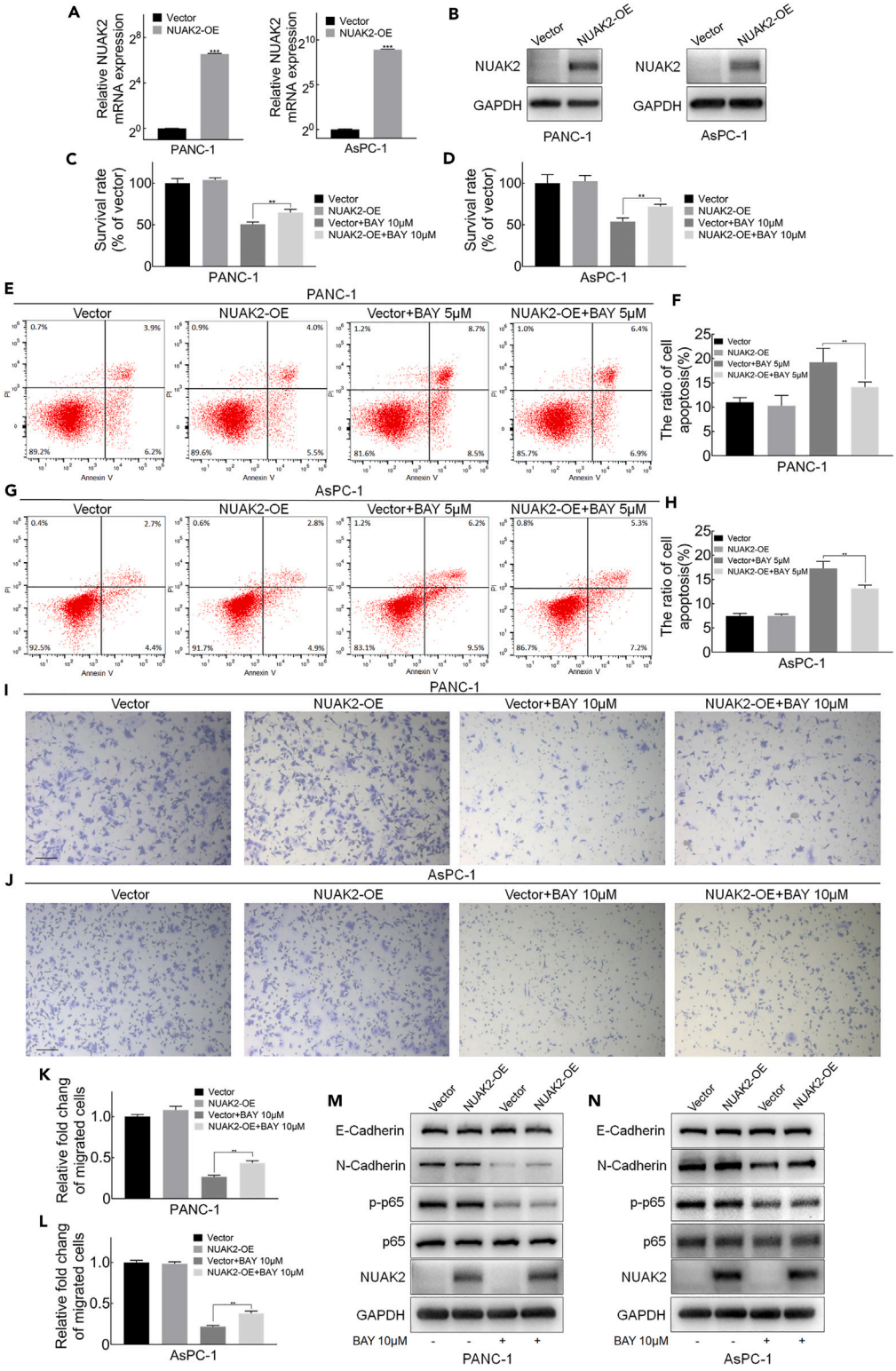

Figure 3. NUAK2 overexpression partially reversed the anti-tumor effect of NF-κB inhibitor in pancreatic cancer cells

(A) High level of NUAK2 mRNA was measured by qRT-PCR. The gene was normalized to GAPDH.

(B) PANC-1 and AsPC-1 cells were transfected with NUAK2 overexpression plasmid. Western blot analysis was performed with NUAK2 and GAPDH antibodies. GAPDH was used as the loading control.

Figure 3. *Continued*

(C and D) PANC-1 and AsPC-1 cells were transfected with vector or NUAK2 overexpression plasmid then exposed to 10 μM BAY11-7082 for 24h. The survival rates of cells were determined by CCK-8 assay.

(E–H) Apoptosis was analyzed by flow cytometry stained with Annexin V/PI after transfected with vector or NUAK2 overexpression plasmid then exposed to 5 μM BAY11-7082 for 18h.

(I–L) The cell migration ability were measured using transwell migration assays after transfected with vector or NUAK2 overexpression plasmid then exposed to 10 μM BAY11-7082 for 20h. Scale bar: 100 μm.

(M and N) The expression of N-cadherin, E-cadherin, p-p65, p65, NUAK2 was examined in PANC-1 and AsPC-1 cells after transfected with vector or NUAK2 overexpression plasmid then exposed to 10 μM BAY11-7082 for 24h by using western blotting analysis. GAPDH was used as loading control. Data are presented as the mean ± SEM, **p < 0.01, ***p < 0.001. Statistical analysis was performed using Student's *t* test.

NUAK2 targets and observed altered mRNA levels of certain genes (Figures 5A and 5B). Given the decreased mRNA levels of Snail1, SMAD2, SMAD3, Fibronectin (FN1), and N-cadherin in Si-NUAK2-transfected cells, we speculated that the effect of NUAK2 on pancreatic cancer might be linked to the regulation of SMAD pathways. Western blotting confirmed that *p*-SMAD2, *p*-SMAD3, SMAD2, SMAD3, FN1, Snail1, and N-cadherin were downregulated in the cells transfected with Si-NUAK2 (Figure 5C). There was no change in total SMAD4 protein expression in SW1990 cells. SMAD4 was not detected in BxPC-3 cells, which was an SMAD4-negative cell line (Figure 5C).

Phosphorylated SMAD2 and SMAD3 have been reported to interact with SMAD4 to form the SMAD2/3/4 complex, which translocates to the nucleus to regulate target gene transcription.[35,36] To determine the specific mechanism of NUAK2 in pancreatic cancer cells, we separated nuclear and cytoplasmic proteins. Less SMAD4 was detected in the nuclear components of Si-NUAK2 transfected cells, but more SMAD4 was detected in the cytoplasm (Figure 5D). These results indicated that NUAK2 knockdown hindered SMAD4 translocation into the nucleus.

The absence of SMAD4 in the BxPC-3 cell line suggested an alternative mechanism existed. A recent study showed that SMAD2/3 mediates oncogenic effects in SMAD4-negative pancreatic cancer by influencing FAK signaling.[37] Immunoblot analysis revealed decreased expression of *p*-FAK and *p*-paxillin (*p*-PXN) in BxPC-3 cells transfected with Si-NUAK2 (Figure 5E). We further overexpressed SMAD4 in SMAD4-negative pancreatic cancer cells and knocked down SMAD4 in SMAD4-positive pancreatic cancer cells to confirm the mechanism of NUAK2 knockdown. The silence of NUAK2 reduced *p*-FAK and *p*-PXN expression in SW1990 cells with SMAD4 knockdown (Figure 5F). In BxPC-3 cells with SMAD4 overexpression, less SMAD4 was detected in the nuclear components of cells transfected with Si-NUAK2 (Figure 5G). The results confirmed the impact of NUAK2 knockdown on SMAD4 translocation. Co-immunoprecipitation assays were performed to explore the relationship between NUAK2 and SMAD2/3. The results demonstrated that NUAK2 could bind to SMAD3 but not SMAD2 (Figure 5H). Regardless of the SMAD4 mutation, we found that NUAK2 mediated oncogenic effects in pancreatic cancer by targeting SMAD2/3.

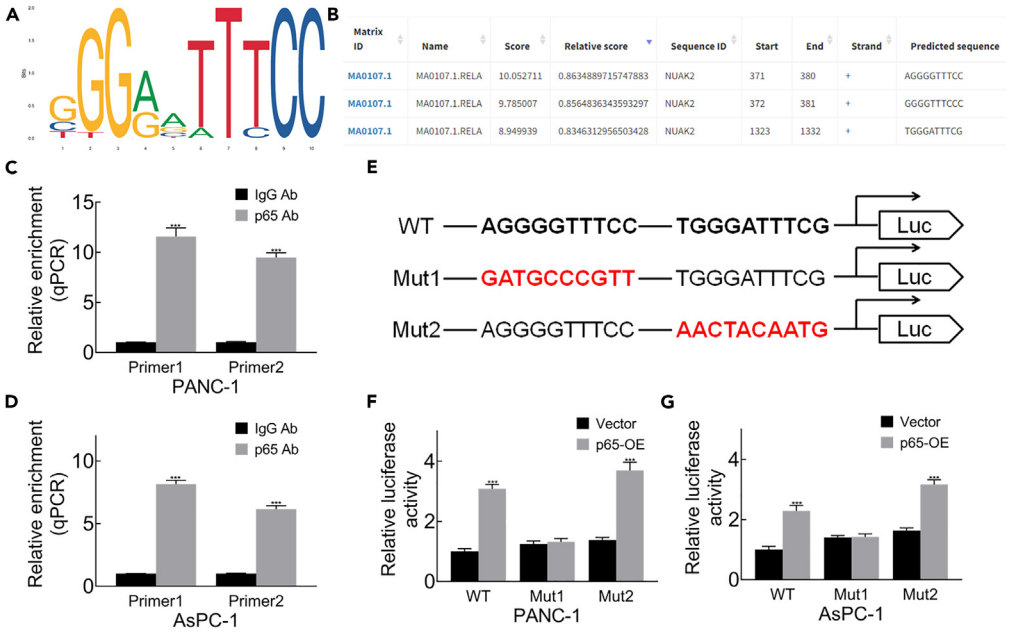

Figure 4. NUAK2 was transcriptionally regulated by NF-κB

(A and B) JASPAR database showed potential binding of p65 to the NUAK2 promoter region.

(C and D) ChIP-qPCR was performed with an anti-p65 antibody in PANC-1 and AsPC-1 cells.

(E) Schematic of the NUAK2 gene promoter. Two potential p65 binding sites and the design of mutants for the binding sites are shown.

(F and G) Dual luciferase assays were performed to confirm the binding site of p65 to the NUAK2 promoter region in PANC-1 and AsPC-1 cells. Data are presented as the mean ± SEM, *p < 0.05, **p < 0.01, ***p < 0.001. Statistical analysis was performed using Student's *t* test.

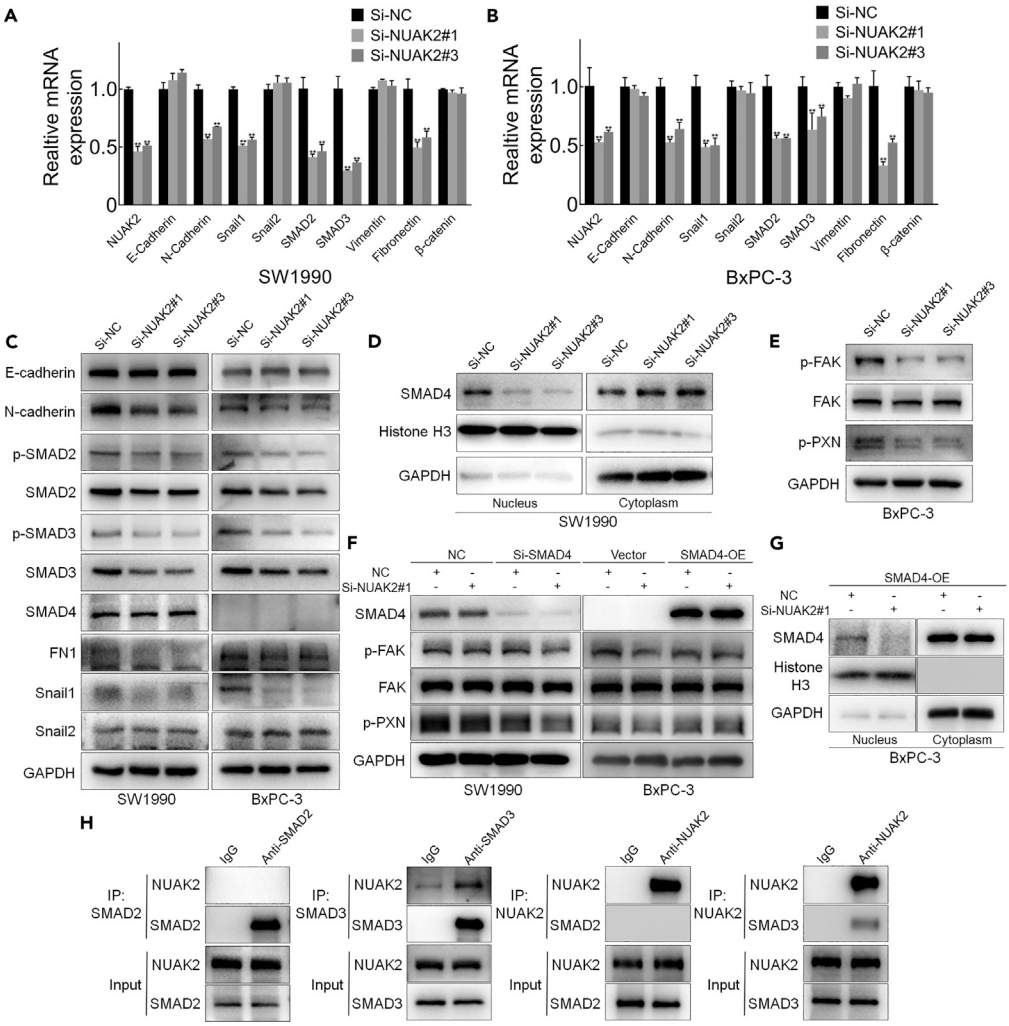

Figure 5. NUAK2 mediated oncogenic effects in pancreatic cancer by targeting SMAD2/3

(A and B) The relative mRNA expression was measured by qRT-PCR. The genes were normalized to GAPDH.

(C) SW1990 and BxPC-3 cells were transfected with Si-NUAK2 and Si-NC. Western blot analysis was performed with E-cadherin, N-cadherin, *p*-SMAD2, *p*-SMAD3, SMAD2, SMAD3, SMAD4, FN1, Snail1, Snail2, and GAPDH. GAPDH was used as the loading control.

(D) SW1990 cells were transfected with Si-NUAK2 and Si-NC. Nuclear and cytoplasmic proteins were extracted from SW1990 cells transfected with Si-NC or Si-NUAK2. GAPDH was used as the loading control for the cytoplasmic extracts, and histone H3 was used as the loading control for the nuclear extracts.

(E) BxPC-3 cells were transfected with Si-NUAK2 and Si-NC. Western blot analysis was performed with *p*-FAK, FAK, *p*-PXN and GAPDH antibodies. GAPDH was used as the loading control.

(F) SW1990 and BxPC-3 cells were transfected with various siRNA as indicated. Western blot analysis was performed with SMAD4, *p*-FAK, FAK, *p*-PXN and GAPDH antibodies. GAPDH was used as the loading control.

(G) BxPC-3 cells were transfected with SMAD4 overexpression plasmid. Nuclear and cytoplasmic proteins were extracted from BxPC-3 cells transfected with Si-NC or Si-NUAK2. GAPDH was used as the loading control for the cytoplasmic extracts, and histone H3 was used as the loading control for the nuclear extracts.

(H) Immunoprecipitation results showed that NUAK2 could bind to SMAD3 but not SMAD2. Data are presented as the mean ± SEM, *p < 0.05, **p < 0.01. Statistical analysis was performed using Student's *t* test.

NUAK2 silencing inhibited pancreatic cancer growth *in vivo*

To further validate the role of NUAK2 in pancreatic cancer tumor growth *in vivo*, a xenograft mouse model was constructed. BxPC-3 cells were stably transfected with Sh-NC or Sh-NUAK2, and the knockdown efficiency was confirmed using qRT-PCR and western blotting (Figures 6A and 6B). The Sh-NUAK2 group exhibited lower tumor weight and volume compared to the control group (Figures 6C–6E). IHC staining revealed significant reductions in NUAK2, Ki-67, SMAD2, and SMAD3 levels following NUAK2 knockdown (Figure 6F). These findings strongly suggested that silencing NUAK2 inhibited the formation of subcutaneous xenograft tumors.

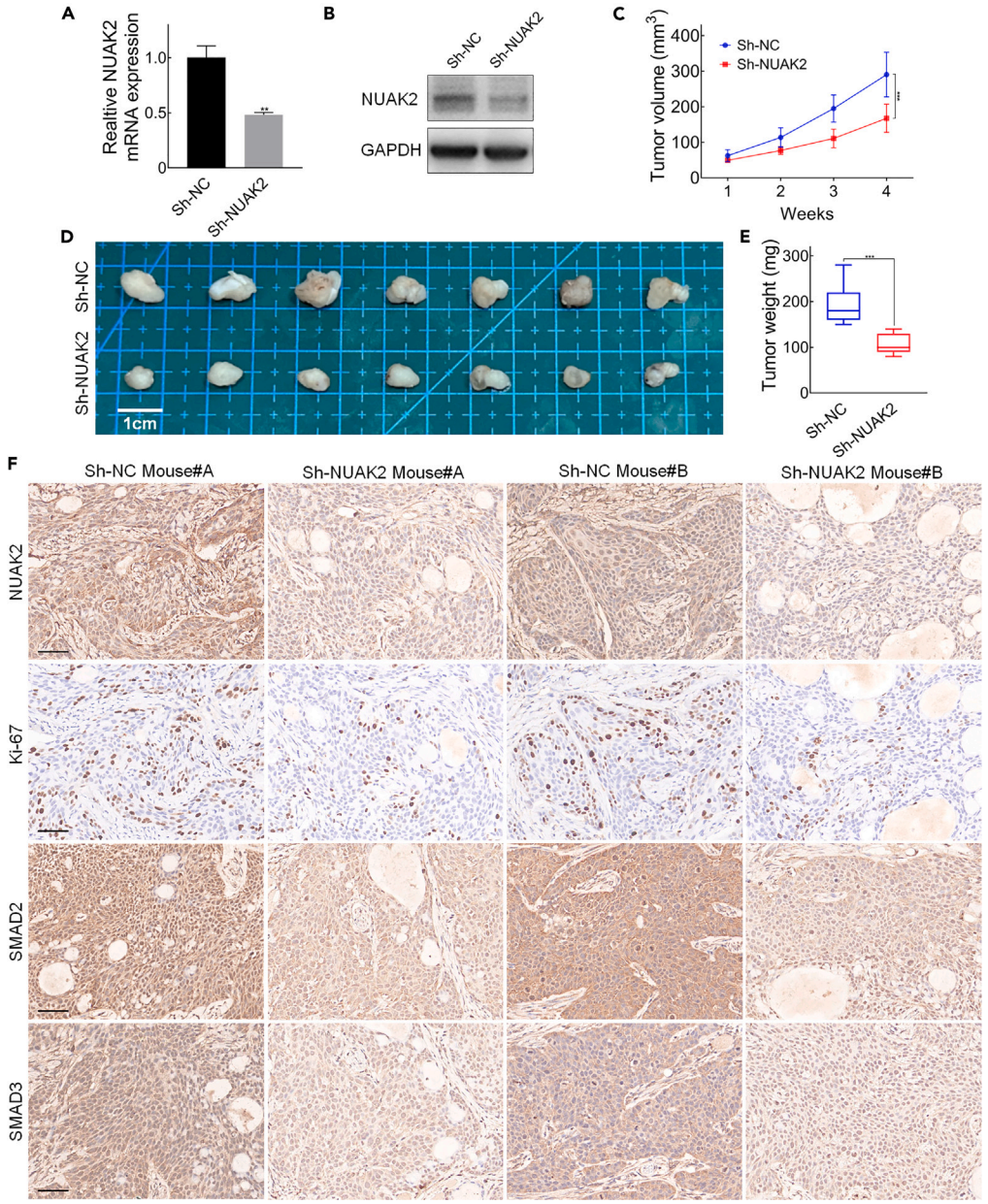

Figure 6. NUAK2 silencing inhibited pancreatic cancer growth in vivo

(A) NUAK2 mRNA was measured by qRT-PCR. The gene was normalized to GAPDH.

(B) BxPC-3 cells were transfected with Sh-NUAK2 and Sh-NC. Western blot analysis was performed with NUAK2 and GAPDH antibodies. GAPDH was used as the loading control.

(C) Tumor growth curves were drawn according to the measured tumor volumes at indicated time points.

(D) Representative images of subcutaneous xenograft tumors.

(E) Tumors from Sh-NC or Sh-NUAK2 group were isolated from nude mice and tumor weight was measured. A box-plot is presented for tumor weight.

(F) Representative IHC staining image of NUAK2, Ki-67, SMAD2, and SMAD3 were acquired on subcutaneous xenograft tumor sections from Sh-NC or Sh-NUAK2 group. Scale bar: 50 μm. The results are presented as the mean ± SEM for each group (n = 7). **p < 0.01, ***p < 0.001. Statistical analysis was performed using Student's *t* test.

NUAK2 silencing enhanced the sensitivity of pancreatic cancer cells to gemcitabine

We then investigated the role of NUAK2 in the treatment of pancreatic cancer, particularly exploring whether NUAK2 silencing could enhance the antitumor effect of gemcitabine, a widely used chemotherapy for pancreatic cancer. CCK-8 assay results demonstrated that silencing NUAK2 heightened the sensitivity of pancreatic cancer cells to gemcitabine (Figures 7A and 7B). Flow cytometry analysis further revealed

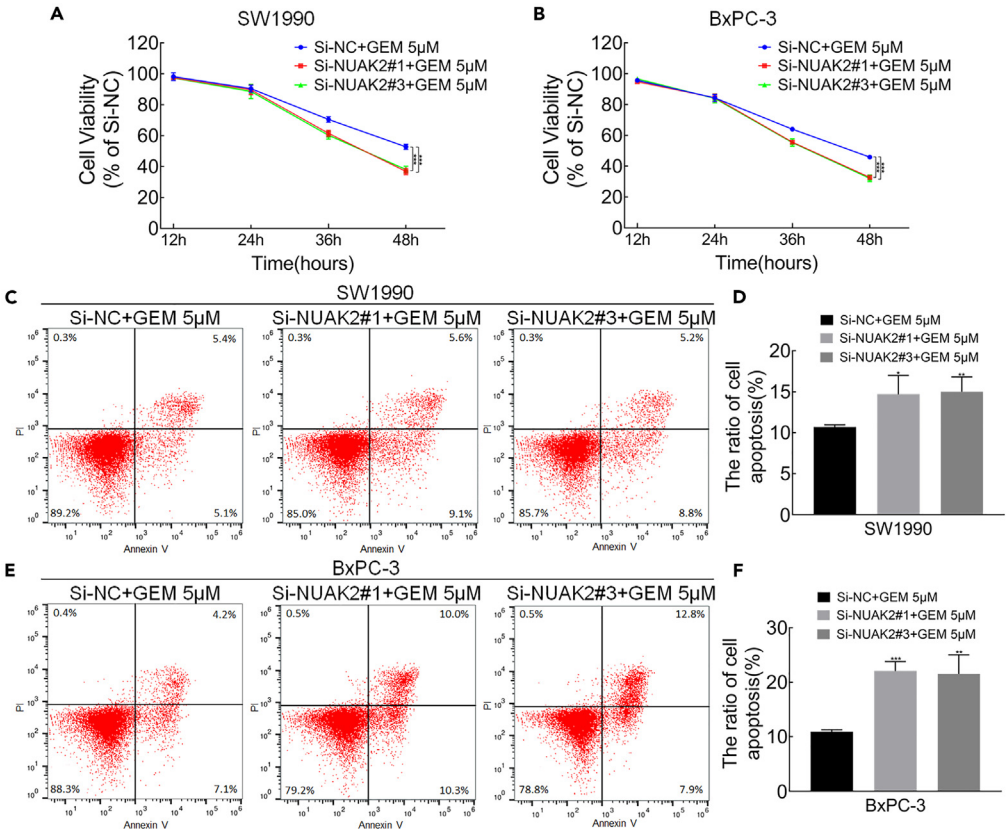

Figure 7. NUAK2 silencing enhanced the sensitivity of pancreatic cancer cells to gemcitabine

(A and B) SW1990 and BxPC-3 cells transfected with Si-NC and Si-NUAK2 were treated with gemcitabine for 24h, 36h, and 48h. The survival rates of cells were determined by CCK-8 assay.

(C–F) Apoptosis was analyzed by flow cytometry stained with Annexin V/PI after exposed to 5 μM gemcitabine for 36h. Data are presented as the mean ± SEM, *p < 0.05, **p < 0.01, ***p < 0.001. Statistical analysis was performed using Student's *t* test.

that gemcitabine resulted in much more apoptosis when NUAK2 was knocked down (Figures 7C–7F). These findings suggested that the knockdown of NUAK2 enhanced the inhibition of SW1990 and BxPC-3 cell viability and induced apoptosis compared to treatment with gemcitabine alone.

DISCUSSION

Pancreatic cancer, characterized by poor prognosis and high mortality, lacks effective curative strategies despite advancements in treatments. Owing to these, there is an urgent need to explore further the new molecular mechanisms of pancreatic cancer progression.

NUAK2, an AMPK-related kinase widely expressed in human tissues, has been reported to be frequently amplified in several human cancers and is considered essential for cancer development.[24] While recent studies have shown that NUAK2's critical roles in liver and prostate cancers, its specific function in pancreatic cancer has remained unclear.[38,39] To address this gap, we initiated an investigation into the functional role of NUAK2 in pancreatic cancer cells by employing siRNA to target NUAK2. Our findings showed that NUAK2 knockdown inhibited the proliferation of pancreatic cancer cells, reduced their ability to migrate and invade, and induced apoptosis. In addition, NUAK2 knockdown also inhibited the formation of subcutaneous xenograft tumors. All these results suggested that NUAK2 silencing had antitumor effects on pancreatic cancer both *in vitro* and *in vivo*.

The nuclear transcription factor NF-κB was initially identified as a nuclear protein interacting with a defined site in the kappa immunoglobulin enhancer.[40] Subsequent studies revealed that the NF-κB pathway is integral to the physiological functions of various cell types, regulating the expression of several important target genes.[41] Activation of the NF-κB pathway is observed in multiple cancers and plays a role in their occurrence and progression.[42] In pancreatic cancer, NF-κB has been implicated in processes such as proliferation, invasion, and metastasis.[13,14] Furthermore, a prior study has indicated that the regulation of NUAK2 depends on the activation of NF-κB.[25]

To inhibit the phosphorylation of NF-κB, we employed BAY11-7082 in this study. Our results demonstrated that BAY11-7082 significantly inhibited the viability, migration, and invasion of pancreatic cancer cells while inducing apoptosis. Notably, BAY11-7082 also led to the downregulation of N-cadherin and NUAK2 expression. Additionally, mRNA and protein levels of NUAK2 were observed to be decreased in p65

knockdown pancreatic cancer cells. These findings strongly suggested that NUAK2 might be regulated by the activation of NF-κB in pancreatic cancer.

To clarify the relationship between NF-κB and NUAK2 in pancreatic cancer, we overexpressed NUAK2 in pancreatic cancer cells. The results indicated that cells overexpressing NUAK2 demonstrated a partial resistance to apoptosis induced by the NF-κB inhibitor, and they also reversed the inhibitory effect of the NF-κB inhibitor on cell migration. However, in a rescue experiment, NUAK2-MUT expression could not reverse the effects of BAY11-7082 on pancreatic cancer cells. This implied that NUAK2 kinase activity was crucial for restoring the antitumor effects of the NF-κB inhibitor. Further investigations were then conducted to explore whether NF-κB acted as the transcription factor promoting NUAK2 transcription. The potential binding sites of p65 on the NUAK2 promoters were verified using ChIP-qPCR and dual luciferase assay. These results indicated that p65 promoted the transcription of NUAK2 by directly binding to the promoter of NUAK2 in pancreatic cancer cells.

We further intended to identify the molecular mechanisms underlying the role of NUAK2 in pancreatic cancer. Recent studies have found links between NUAK2 and the TGF-β signaling pathway. TGF-β signaling pathways are known to regulate cell proliferation, migration, and apoptosis, playing a crucial role in the tumorigenesis of pancreatic cancer. The canonical TGF-β signaling pathway is mediated by SMAD transcription factors.[43] Given the observed reduction in SMAD2/3 mRNA levels in Si-NUAK2 transfected cells and the known association between the TGF-β signal and NUAK2, we speculated that the effect of NUAK2 on pancreatic cancer might be related to the regulation of SMAD pathways. The results indicated a significant decrease in the expression levels of *p*-SMAD2, *p*-SMAD3, SMAD2, and SMAD3 upon silencing NUAK2. The translocation of the SMAD2/3/4 complex into the nucleus depends on the interaction of phosphorylated SMAD2 and SMAD3 with SMAD4.[35,36] To further clarify the regulation of SMAD4 expression, proteins were extracted from the nucleus and cytoplasm. Our findings demonstrated that NUAK2 knockdown decreased the translocation of SMAD4 into the nucleus, explaining the antitumor effect of NUAK2 silencing.

However, it is worth noting that the potential targeted molecule, SMAD4, is negative in the BxPC-3 cell line. SMAD4 deficiency is a common occurrence in pancreatic cancer and is associated with poor overall survival.[44] Recognizing the likelihood of other mechanisms in BxPC-3 cells, the current study focused on the regulation of SMAD2/3 in SMAD4-negative pancreatic cancer. Previous research has indicated that SMAD2/3 mediates oncogenic effects in SMAD4-negative pancreatic cancer by influencing FAK signaling.[37] Consistent with this, we also observed a decreased expression of *p*-PXN and *p*-FAK in BxPC-3 cells following NUAK2 knockdown. To validate the mechanism underlying NUAK2 knockdown, we conducted experiments involving the overexpression of SMAD4 in SMAD4-negative pancreatic cancer cells and knocked down SMAD4 in SMAD4-positive pancreatic cancer cells. The results demonstrated that in the presence of SMAD4, pancreatic cancer cells with NUAK2 knockdown tended to reduce the translocation of SMAD4 into the nucleus. In the absence of SMAD4, the effects of NUAK2 knockdown appeared to be mediated by FAK signaling. The relationship between NUAK2 and SMAD2/3 was further confirmed through co-immunoprecipitation, revealing that NUAK2 could bind to SMAD3 but not to SMAD2. These findings collectively suggested that NUAK2 mediated oncogenic effects in pancreatic cancer by targeting SMAD2/3 regardless of SMAD4 deficiency.

Several studies have highlighted the involvement of the SMAD pathway in mediating gemcitabine resistance.[45,46] Additional studies have demonstrated that inhibiting TGF-β signaling enhances the chemosensitivity of intrahepatic cholangiocarcinoma to gemcitabine in the patient-derived xenograft (PDX) models.[47] Concurrently, thymoquinone has been found to augment sensitivity to gemcitabine in pancreatic cancer cells through the TGFβ/SMAD pathway.[48] Building on these findings, we explored the role of NUAK2 in the gemcitabine treatment of pancreatic cancer cells. Our results showed that silencing NUAK2 heightened the sensitivity of pancreatic cancer cells to gemcitabine, suggesting that targeting NUAK2 could be an attractive therapeutic approach for pancreatic cancer. Notably, various NUAK-targeting inhibitors have been recently developed.[49] Some of them demonstrate effectiveness against human cancers.[38,50] Consequently, NUAK2 inhibitors hold substantial promise in pancreatic cancer treatment. In the future, we plan to conduct both clinical and basic studies on these inhibitors to offer guidance for the treatment of pancreatic cancer.

In conclusion, our research revealed that NUAK2 is subject to regulation by NF-κB activation in pancreatic cancer. Silencing NUAK2 exhibited antitumor effects in pancreatic cancer by targeting SMAD2/3, irrespective of SMAD4 deficiency. Furthermore, our findings showed that NUAK2 silencing heightened the sensitivity of pancreatic cancer cells to gemcitabine treatment, implying that NUAK2 inhibitors could emerge as a promising treatment strategy for pancreatic cancer.

Limitations of the study

The mechanism via which NUAK2 regulates the FAK pathway in SMAD4-negative pancreatic cancer cells remains unclear and warrants further investigation. Additionally, for a comprehensive understanding of the potential therapeutic implications of NUAK2 inhibition in clinical treatments, small molecule inhibitors with high specificity should be used to evaluate pancreatic cancer treatments.

STAR★METHODS

Detailed methods are provided in the online version of this paper and include the following:

- KEY RESOURCES TABLE
- RESOURCE AVAILABILITY
  - Lead contact
  - Materials availability

SUPPLEMENTAL INFORMATION

Supplemental information can be found online at https://doi.org/10.1016/j.isci.2024.109406.

ACKNOWLEDGMENTS

This work was supported by the National Natural Science Foundation of China (82272917, 81972258, 82103016, and 82203158), National High Level Hospital Clinical Research Funding (2022-PUMCH-A-133, 2022-PUMCH-B-004, 2022-PUMCH-D-001, and 2022-PUMCH-A-245), CAMS Innovation Fund for Medical Sciences (2021-1-I2M-002), and National Multidisciplinary Cooperative Diagnosis and Treatment Capacity Building Project for Major Diseases.

AUTHOR CONTRIBUTIONS

R.W. and D.S. conducted most of the experiments. R.W. and D.S. wrote the main manuscript. T.Z. conceived the original idea and supervised the project. Y.L., H.H., J.Q., Z.C., and G.Y. conducted statistical analysis and prepared figures. H.C., J.T., W.L., and G.W. assisted the experiments. All authors reviewed the manuscript and approved the final manuscript.

DECLARATION OF INTERESTS

The authors declare no competing interests.

Received: August 25, 2023
Revised: January 13, 2024
Accepted: February 29, 2024
Published: March 4, 2024

REFERENCES

1. Rahib, L., Wehner, M.R., Matrisian, L.M., and Nead, K.T. (2021). Estimated Projection of US Cancer Incidence and Death to 2040. JAMA Netw. Open *4*, e214708. https://doi.org/10.1001/jamanetworkopen.2021.4708.
2. Siegel, R.L., Miller, K.D., Wagle, N.S., and Jemal, A. (2023). Cancer statistics, 2023. CA A Cancer J. Clin. *73*, 17–48. https://doi.org/10.3322/caac.21763.
3. Mizrahi, J.D., Surana, R., Valle, J.W., and Shroff, R.T. (2020). Pancreatic cancer. Lancet *395*, 2008–2020. https://doi.org/10.1016/S0140-6736(20)30974-0.
4. Wood, L.D., Canto, M.I., Jaffee, E.M., and Simeone, D.M. (2022). Pancreatic Cancer: Pathogenesis, Screening, Diagnosis, and Treatment. Gastroenterology *163*, 386–402.e1. https://doi.org/10.1053/j.gastro.2022.03.056.
5. Hoesel, B., and Schmid, J.A. (2013). The complexity of NF-kappaB signaling in inflammation and cancer. Mol. Cancer *12*, 86. https://doi.org/10.1186/1476-4598-12-86.
6. Amit, S., and Ben-Neriah, Y. (2003). NF-kappaB activation in cancer: a challenge for ubiquitination- and proteasome-based therapeutic approach. Semin. Cancer Biol. *13*, 15–28. https://doi.org/10.1016/s1044-579x(02)00096-2.
7. Lenardo, M., Pierce, J.W., and Baltimore, D. (1987). Protein-binding sites in Ig gene enhancers determine transcriptional activity and inducibility. Science *236*, 1573–1577. https://doi.org/10.1126/science.3109035.
8. Silke, J., and O'Reilly, L.A. (2021). NF-kappaB and Pancreatic Cancer; Chapter and Verse. Cancers *13*, 4510. https://doi.org/10.3390/cancers13184510.
9. Ben-Neriah, Y., and Karin, M. (2011). Inflammation meets cancer, with NF-kappaB

as the matchmaker. Nat. Immunol. *12*, 715–723. https://doi.org/10.1038/ni.2060.
10. Taniguchi, K., and Karin, M. (2018). NF-kappaB, inflammation, immunity and cancer: coming of age. Nat. Rev. Immunol. *18*, 309–324. https://doi.org/10.1038/nri.2017.142.
11. Lu, T., Sathe, S.S., Swiatkowski, S.M., Hampole, C.V., and Stark, G.R. (2004). Secretion of cytokines and growth factors as a general cause of constitutive NFkappaB activation in cancer. Oncogene *23*, 2138–2145. https://doi.org/10.1038/sj.onc.1207332.
12. Kabacaoglu, D., Ruess, D.A., Ai, J., and Algül, H. (2019). NF-kappaB/Rel Transcription Factors in Pancreatic Cancer: Focusing on RelA, c-Rel, and RelB. Cancers *11*, 937. https://doi.org/10.3390/cancers11070937.
13. Zhuang, Z., Ju, H.Q., Aguilar, M., Gocho, T., Li, H., Iida, T., Lee, H., Fan, X., Zhou, H., Ling, J., et al. (2016). IL1 Receptor Antagonist Inhibits Pancreatic Cancer Growth by Abrogating NF-kappaB Activation. Clin. Cancer Res. *22*, 1432–1444. https://doi.org/10.1158/1078-0432.CCR-14-3382.
14. Nomura, A., Majumder, K., Giri, B., Dauer, P., Dudeja, V., Roy, S., Banerjee, S., and Saluja, A.K. (2016). Inhibition of NF-kappa B pathway leads to deregulation of epithelial-mesenchymal transition and neural invasion in pancreatic cancer. Lab. Invest. *96*, 1268–1278. https://doi.org/10.1038/labinvest.2016.109.
15. Wang, S.J., Sun, B., Cheng, Z.X., Zhou, H.X., Gao, Y., Kong, R., Chen, H., Jiang, H.C., Pan, S.H., Xue, D.B., and Bai, X.W. (2011). Dihydroartemisinin inhibits angiogenesis in pancreatic cancer by targeting the NF-kappaB pathway. Cancer Chemother. Pharmacol. *68*, 1421–1430. https://doi.org/10.1007/s00280-011-1643-7.
16. Yu, C., Chen, S., Guo, Y., and Sun, C. (2018). Oncogenic TRIM31 confers gemcitabine resistance in pancreatic cancer via activating the NF-kappaB signaling pathway. Theranostics *8*, 3224–3236. https://doi.org/10.7150/thno.23259.
17. Gamble, C., McIntosh, K., Scott, R., Ho, K.H., Plevin, R., and Paul, A. (2012). Inhibitory kappa B Kinases as targets for pharmacological regulation. Br. J. Pharmacol. *165*, 802–819. https://doi.org/10.1111/j.1476-5381.2011.01608.x.
18. Pramanik, K.C., Makena, M.R., Bhowmick, K., and Pandey, M.K. (2018). Advancement of NF-kappaB Signaling Pathway: A Novel Target in Pancreatic Cancer. Int. J. Mol. Sci. *19*, 3890. https://doi.org/10.3390/ijms19123890.
19. Li, Q., Yang, G., Feng, M., Zheng, S., Cao, Z., Qiu, J., You, L., Zheng, L., Hu, Y., Zhang, T., and Zhao, Y. (2018). NF-kappaB in pancreatic cancer: Its key role in chemoresistance. Cancer Lett. *421*, 127–134. https://doi.org/10.1016/j.canlet.2018.02.011.
20. Sun, X., Gao, L., Chien, H.Y., Li, W.C., and Zhao, J. (2013). The regulation and function of the NUAK family. J. Mol. Endocrinol. *51*, R15–R22. https://doi.org/10.1530/JME-13-0063.
21. Koh, H.J., Toyoda, T., Fujii, N., Jung, M.M., Rathod, A., Middelbeek, R.J.W., Lessard, S.J., Treebak, J.T., Tsuchihara, K., Esumi, H., et al. (2010). Sucrose nonfermenting AMPK-related kinase (SNARK) mediates contraction-stimulated glucose transport in mouse skeletal muscle. Proc. Natl. Acad. Sci. USA *107*, 15541–15546. https://doi.org/10.1073/pnas.1008131107.
22. Namiki, T., Tanemura, A., Valencia, J.C., Coelho, S.G., Passeron, T., Kawaguchi, M., Vieira, W.D., Ishikawa, M., Nishijima, W., Izumo, T., et al. (2011). AMP kinase-related kinase NUAK2 affects tumor growth, migration, and clinical outcome of human melanoma. Proc. Natl. Acad. Sci. USA *108*, 6597–6602. https://doi.org/10.1073/pnas.1007694108.
23. Rune, A., Osler, M.E., Fritz, T., and Zierath, J.R. (2009). Regulation of skeletal muscle sucrose, non-fermenting 1/AMP-activated protein kinase-related kinase (SNARK) by metabolic stress and diabetes. Diabetologia *52*, 2182–2189. https://doi.org/10.1007/s00125-009-1465-x.
24. Monteverde, T., Muthalagu, N., Port, J., and Murphy, D.J. (2015). Evidence of cancer-promoting roles for AMPK and related kinases. FEBS J. *282*, 4658–4671. https://doi.org/10.1111/febs.13534.
25. Legembre, P., Schickel, R., Barnhart, B.C., and Peter, M.E. (2004). Identification of SNF1/AMP kinase-related kinase as an NF-kappaB-regulated anti-apoptotic kinase involved in CD95-induced motility and invasiveness. J. Biol. Chem. *279*, 46742–46747. https://doi.org/10.1074/jbc.M404334200.
26. Zhu, Y., Liu, Z., Wan, Y., Zou, L., Liu, L., Ding, S., Lu, C., and Qiu, F. (2022). PARP14 promotes the growth and glycolysis of acute myeloid leukemia cells by regulating HIF-1alpha expression. Clin. Immunol. *242*, 109094. https://doi.org/10.1016/j.clim.2022.109094.
27. Wang, G., Wang, J., Li, X., Wu, Q., Yao, R., and Luo, X. (2023). Hypoxia and TNF-alpha Synergistically Induce Expression of IL-6 and IL-8 in Human Fibroblast-like Synoviocytes via Enhancing TAK1/NF-kappaB/HIF-1alpha Signaling. Inflammation *46*, 912–924. https://doi.org/10.1007/s10753-022-01779-x.
28. Cui, X., Wang, Y., Lan, W., Wang, S., Cui, Y., Zhang, X., Lin, Z., and Piao, J. (2022). SPOCK1 promotes metastasis in pancreatic cancer via NF-kappaB-dependent epithelial-mesenchymal transition by interacting with IkappaB-alpha. Cell. Oncol. *45*, 69–84. https://doi.org/10.1007/s13402-021-00652-7.
29. Bonnard, C., Navaratnam, N., Ghosh, K., Chan, P.W., Tan, T.T., Pomp, O., Ng, A.Y.J., Tohari, S., Changede, R., Carling, D., et al. (2020). A loss-of-function NUAK2 mutation in humans causes anencephaly due to impaired Hippo-YAP signaling. J. Exp. Med. *217*, e20191561. https://doi.org/10.1084/jem.20191561.
30. Kolliopoulos, C., Raja, E., Razmara, M., Heldin, P., Heldin, C.H., Moustakas, A., and van der Heide, L.P. (2019). Transforming growth factor beta (TGFbeta) induces NUAK kinase expression to fine-tune its signaling output. J. Biol. Chem. *294*, 4119–4136. https://doi.org/10.1074/jbc.RA118.004984.
31. van de Vis, R.A.J., Moustakas, A., and van der Heide, L.P. (2021). NUAK1 and NUAK2 Fine-Tune TGF-beta Signaling. Cancers *13*, 3377. https://doi.org/10.3390/cancers13133377.
32. Ikushima, H., and Miyazono, K. (2010). TGFbeta signalling: a complex web in cancer progression. Nat. Rev. Cancer *10*, 415–424. https://doi.org/10.1038/nrc2853.
33. Pardali, E., Goumans, M.J., and ten Dijke, P. (2010). Signaling by members of the TGF-beta family in vascular morphogenesis and disease. Trends Cell Biol. *20*, 556–567. https://doi.org/10.1016/j.tcb.2010.06.006.
34. Wu, M.Y., and Hill, C.S. (2009). Tgf-beta superfamily signaling in embryonic development and homeostasis. Dev. Cell *16*, 329–343. https://doi.org/10.1016/j.devcel.2009.02.012.
35. Massagué, J., Seoane, J., and Wotton, D. (2005). Smad transcription factors. Genes Dev. *19*, 2783–2810. https://doi.org/10.1101/gad.1350705.
36. Gough, N.R., Xiang, X., and Mishra, L. (2021). TGF-beta Signaling in Liver, Pancreas, and Gastrointestinal Diseases and Cancer. Gastroenterology *161*, 434–452.e15. https://doi.org/10.1053/j.gastro.2021.04.064.
37. Bertrand-Chapel, A., Caligaris, C., Fenouil, T., Savary, C., Aires, S., Martel, S., Huchedé, P., Chassot, C., Chauvet, V., Cardot-Ruffino, V., et al. (2022). SMAD2/3 mediate oncogenic effects of TGF-beta in the absence of SMAD4. Commun. Biol. *5*, 1068. https://doi.org/10.1038/s42003-022-03994-6.
38. Yuan, W.C., Pepe-Mooney, B., Galli, G.G., Dill, M.T., Huang, H.T., Hao, M., Wang, Y., Liang, H., Calogero, R.A., and Camargo, F.D. (2018). NUAK2 is a critical YAP target in liver cancer. Nat. Commun. *9*, 4834. https://doi.org/10.1038/s41467-018-07394-5.
39. Fu, W., Zhao, M.T., Driver, L.M., Schirmer, A.U., Yin, Q., You, S., Freedland, S.J., DiGiovanni, J., Drewry, D.H., and Macias, E. (2022). NUAK family kinase 2 is a novel therapeutic target for prostate cancer. Mol. Carcinog. *61*, 334–345. https://doi.org/10.1002/mc.23374.
40. Sen, R., and Baltimore, D. (1986). Inducibility of kappa immunoglobulin enhancer-binding protein Nf-kappa B by a posttranslational mechanism. Cell *47*, 921–928. https://doi.org/10.1016/0092-8674(86)90807-x.
41. May, M.J., and Ghosh, S. (1998). Signal transduction through NF-kappa B. Immunol. Today *19*, 80–88. https://doi.org/10.1016/s0167-5699(97)01197-3.
42. Deka, K., and Li, Y. (2023). Transcriptional Regulation during Aberrant Activation of NF-kappaB Signalling in Cancer. Cells *12*. https://doi.org/10.3390/cells12050788.
43. Mazi, F.A., Cakiroglu, E., Uysal, M., Kalyoncu, M., Demirci, D., Sozeri, P.Y.G., Yilmaz, G.O., Ozhan, S.E., and Senturk, S. (2023). The paracaspase MALT1 is a downstream target of Smad3 and potentiates the crosstalk between TGF-beta and NF-kB signaling pathways in cancer cells. Cell. Signal. *105*, 110611. https://doi.org/10.1016/j.cellsig.2023.110611.
44. Wang, J.D., Jin, K., Chen, X.Y., Lv, J.Q., and Ji, K.W. (2017). Clinicopathological significance of SMAD4 loss in pancreatic ductal adenocarcinomas: a systematic review and meta-analysis. Oncotarget *8*, 16704–16711. https://doi.org/10.18632/oncotarget.14335.
45. Zhuang, J., Shen, L., Yang, L., Huang, X., Lu, Q., Cui, Y., Zheng, X., Zhao, X., Zhang, D., Huang, R., et al. (2017). TGFbeta1 Promotes Gemcitabine Resistance through Regulating the LncRNA-LET/NF90/miR-145 Signaling Axis in Bladder Cancer. Theranostics *7*, 3053–3067. https://doi.org/10.7150/thno.19542.
46. Hussain, S.M., Kansal, R.G., Alvarez, M.A., Hollingsworth, T.J., Elahi, A., Miranda-Carboni, G., Hendrick, L.E., Pingili, A.K., Albritton, L.M., Dickson, P.V., et al. (2021). Role of TGF-beta in pancreatic ductal adenocarcinoma progression and PD-L1 expression. Cell. Oncol. *44*, 673–687. https://doi.org/10.1007/s13402-021-00594-0.

47. Mancarella, S., Gigante, I., Serino, G., Pizzuto, E., Dituri, F., Valentini, M.F., Wang, J., Chen, X., Armentano, R., Calvisi, D.F., and Giannelli, G. (2022). Crenigacestat blocking notch pathway reduces liver fibrosis in the surrounding ecosystem of intrahepatic CCA viaTGF-beta inhibition. J. Exp. Clin. Cancer Res. *41*, 331. https://doi.org/10.1186/s13046-022-02536-6.

48. Zhao, Z., Liu, L., Chen, H., Li, S., Guo, Y., Hou, X., and Yang, J. (2023). Thymoquinone affects the gemcitabine sensitivity of pancreatic cancer by regulating collagen via hypoxia inducible factor-1alpha. Front. Pharmacol. *14*, 1138265. https://doi.org/10.3389/fphar.2023.1138265.

49. Faisal, M., Kim, J.H., Yoo, K.H., Roh, E.J., Hong, S.S., and Lee, S.H. (2021). Development and Therapeutic Potential of NUAKs Inhibitors. J. Med. Chem. *64*, 2–25. https://doi.org/10.1021/acs.jmedchem.0c00533.

50. Yang, H., Wang, X., Wang, C., Yin, F., Qu, L., Shi, C., Zhao, J., Li, S., Ji, L., Peng, W., et al. (2021). Optimization of WZ4003 as NUAK inhibitors against human colorectal cancer. Eur. J. Med. Chem. *210*, 113080. https://doi.org/10.1016/j.ejmech.2020.113080.

STAR★METHODS

KEY RESOURCES TABLE

REAGENT or RESOURCE	SOURCE	IDENTIFIER
Antibodies		
anti-GAPDH antibody	Ray Antibody	CAT# RM2002
anti-Histone 3 antibody	Ray Antibody	CAT# RM2005
anti-mouse IgG HRP linked antibody	Ray Antibody	CAT# RM3001
anti-rabbit IgG HRP linked antibody	Ray Antibody	CAT# RM3002
anti-N-cadherin antibody	Proteintech	CAT# 22018
anti-E-cadherin antibody	Proteintech	CAT# 20874
anti-SMAD2 antibody	Proteintech	CAT# 12570
anti-SMAD3 antibody	Proteintech	CAT# 66516
anti-p65 antibody	Proteintech	CAT# 10745
anti-Fibronectin antibody	Proteintech	CAT# 66042
anti-NUAK2 antibody	Abcam	CAT# ab126048
anti-Ki-67 antibody	Abcam	CAT# ab16667
anti-NUAK2 antibody	CST	CAT# 15452
anti-*p*-SMAD2 antibody	CST	CAT# 3108
anti-*p*-SMAD3 antibody	CST	CAT# 9520
anti-SMAD2 antibody	CST	CAT# 5339
anti-SMAD3 antibody	CST	CAT# 9523
anti-SMAD4 antibody	CST	CAT# 38454
anti-Snail1 antibody	CST	CAT# 3879
anti-Snail2 antibody	CST	CAT# 9585
anti-*p*-Paxillin antibody	CST	CAT# 2541
anti-*p*-FAK antibody	CST	CAT# 8556
anti-FAK antibody	CST	CAT# 3285
anti-p-p65 antibody	CST	CAT# 3033
anti-p65 antibody	CST	CAT# 8242
Chemicals, peptides, and recombinant proteins		
Gemcitabine	Macklin	CAT# G824361
DMSO	Sigma-Aldrich	CAT# W387520
BAY 11-7082	Aladdin Chemical	CAT# B129693
WZ 4003	Aladdin Chemical	CAT# W275066
TRIzol	Invitrogen	CAT# 15596
Lipofectamine 3000	Invitrogen	CAT# L3000015
Lipofectamine RNAiMAX	Invitrogen	CAT# 13778150
Puromycin	Sigma-Aldrich	CAT# 540411
Crystal Violet Staining Solution	Beyotime	CAT# C0121
Critical commercial assays		
TB Green™ Premix Ex Taq™ II	TaKaRa	CAT# RR820A
Prime-Script™ RT Master Mix	TaKaRa	CAT# RR036A
CCK-8 assay solution	Vazyme	CAT# A311
BeyoClick™ EdU-488 detection kits	Beyotime	CAT# C0071S
Annexin V-FITC/PI Cell Apoptosis Detection Kit	TransGen	CAT# A101

(*Continued on next page*)

Continued

REAGENT or RESOURCE	SOURCE	IDENTIFIER
Nuclear and Cytoplasmic Protein Extraction Kit	Beyotime	CAT# P0028
REAL EnVision Detection Kit	Dako	CAT# K5007
Pierce™ Protein A/G Magnetic Beads	Thermo Fisher Scientific	CAT# 88803
BeyoChIP™ Enzymatic ChIP Assay Kit	Beyotime	CAT# P2083S
Dual Luciferase Reporter Gene Assay Kit	Yeasen	CAT# 11402ES60
Experimental models: Cell lines		
Human: AsPC-1	ATCC	Cat# CRL-1682
Human: BxPC-3	ATCC	Cat# CRL-1687
Human: SW1990	ATCC	Cat# CRL-2172
Human: PANC-1	ATCC	Cat# CRL-1469
Experimental models: Organisms/strains		
Mouse: BALB/c	Vitalstar Biotechnology	N/A
Oligonucleotides		
See Table S1	Tsingke Biotechnology	N/A
Software and algorithms		
GraphPad Prism version 9.0	GraphPad Software	N/A
FlowJo version 10.0	FlowJo Software	N/A

RESOURCE AVAILABILITY

Lead contact

Further information and requests for resources and reagents should be directed to and will be fulfilled by the lead contact, Taiping Zhang (tpingzhang@yahoo.com).

Materials availability

The plasmids used in this study are available from the lead contact. This study did not generate new unique reagents.

Data and code availability

- This paper does not report original code.
- Data reported in this paper will be shared by the lead contact upon request.
- Any additional information required to reanalyze the data reported in this paper is available from the lead contact upon request.

EXPERIMENTAL MODEL AND STUDY PARTICIPANT DETAILS

Mice

All animal experiments were reviewed and approved by the Committee on Ethics of Beijing Vitalstar Biotechnology Company and performed in accordance with the Beijing Laboratory Animal Welfare and Ethical Guidelines of the Beijing Administration Committee of Laboratory Animals (VST-SY-20221122). Six-week-old female nude mice (BALB/c) were purchased from Beijing Vitalstar Biotechnology Company and housed. Mice were maintained under specific pathogen-free (SPF) conditions before the commencement of the experiments.

Cell lines and cell culture

The human pancreatic cancer cell lines (AsPC-1, BxPC-3, SW1990, and PANC-1) were purchased from the American Type Culture Collection. For cell culture, all media were supplemented with 10% fetal bovine serum (Cell Technologies) and 1% penicillin/streptomycin (VivaCell Biosciences). AsPC-1, BxPC-3, and SW1990 cells were grown in RPMI 1640 Medium (VivaCell Biosciences) and PANC-1 cells were culured in Dulbecco's Modified Eagle's Medium (DMEM) (VivaCell Biosciences). All cells were maintained in a humidified atmosphere with 5% carbon dioxide at a temperature of 37°C.

Clinical samples

Tissue samples were collected from patients diagnosed with pancreatic cancer who underwent surgical resection at our department between 2021 and 2023 (Table S2). All participating patients provided informed consent for the collection of tissue samples, and the study was

approved by the Ethics Committee of Peking Union Medical College Hospital (I-23PJ800). Clinical samples were fixed in 4% paraformaldehyde, and paraffin-embedded tissue sections were prepared for subsequent examination.

METHOD DETAILS

RNA extraction and quantitative real-time PCR (qRT-PCR)

Total RNAs from cultured cells were extracted using the TRIzol reagent (Invitrogen) and then subjected to reverse transcription using PrimeScript RT Master Mix (Takara Bio). qPCR was performed with Quantstudio 3 Real-Time PCR System using the TB Green Premix Ex Taq II (Takara Bio). The $2^{-\Delta\Delta Ct}$ method was employed to calculate the relative fold changes in mRNA expression levels, with normalization to the endogenous gene GAPDH. All the primer sequences used in this study are shown in Table S1.

Transfection assay

Human p65, SMAD4, NUAK2, and mutated NUAK2 overexpression plasmids were synthesized and cloned into vectors by Shanghai GeneChem Co., Ltd. (Shanghai, China). An empty plasmid was employed as the negative control. The transfection of plasmids into cells was executed using Lipofectamine 3000 (Invitrogen), according to the manufacturer's instructions.

Small interfering RNA-mediated gene silencing and lentiviral transfection

Scrambled small interfering RNA (siRNA) or target-specific siRNA was employed to interfere with the expression of corresponding targets using Lipofectamine RNAiMAX Reagent (Invitrogen, USA) according to the manufacturer's instructions. Total protein and RNA were extracted 48 h after transfection, and transfection efficiency was assessed through western blotting and qRT-PCR. All the siRNA oligomers were synthesized by Tsingke Biotech Co., Ltd. (Beijing, China). The target sequences for NUAK2 siRNA target sequences were as follows: Si-NUAK2#1, 5'-GCATGACCATAAGATCCTA-3'; Si-NUAK2#2,5'-GGCAAGTTCCTGCAGACAT-3'; Si-NUAK2#3,5'-GCAAGATCTGATGCACATA-3'. For p65 siRNA, the target sequences were: Si-p65#1,5'-GATTGAGGAGAAACGTAAA -3'; Si-p65#2, 5'-AATACACCTCAATGTCCTC-3'. The SMAD4 siRNA target sequence was 5'-CGAGTTGTATCACCTGGAATT-3'.

Lentiviral vectors were obtained from Shanghai Genechem Company (Shanghai, China). NUAK2 shRNA target sequence was 5'-CCGGTGGCTGTTGATGGTGAA-3'. The supernatant from cultured 293T cells was used to infect BxPC-3 cells, and stable cell lines were selected using puromycin (Sigma-Aldrich) for a period of 2 weeks.

Cell viability and cell survival assay

Cells were seeded into 96-well plates, and following transfection or treatments with drugs, they were incubated with CCK-8 assay solution (Vazyme) for 2 h at 37°C according to the manufacturer's protocol. The absorbance was subsequently measured at 450 nm using an automated microplate reader.

5-Ethynyl-20- deoxyuridine (EdU) proliferation assay

The EdU assay was performed following the guidelines provided by the BeyoClick EdU-488 Detection Kit (Beyotime). Cells were initially seeded in 6-well plates and cultured for 24 h. Subsequently, they were incubated with EdU solution at the concentration of 10 μM for 2 h in a cell incubator. Then, cells were fixed in 4% paraformaldehyde, permeabilized with 0.3% Triton, and stained with reaction buffer and Hoechst33342. The observation and photography of cells were carried out under a fluorescence microscope (Olympus).

Transwell migration and invasion assays

The migratory and invasive abilities of pancreatic cancer cells were assessed using the Transwell chamber (8 μm pore size, 24-well plate; Falcon, BD Biosciences, USA). For invasion assays, Matrigel (BD Biosciences) was diluted 1:6 with media, and precoated on the upper surface of the chamber, and allowed to solidify at 37°C for 1h. After 48 h of transfection, cells from each group were collected and resuspended in a serum-free medium. Subsequently, 1×10^5 cells were added to the upper chamber, and the lower chamber was filled with 600 μL of media containing 2–10% fetal bovine serum. After 24 h of incubation, the upper chamber was removed, and the cells were fixed in 4% formaldehyde for 20 min, followed by staining with 0.1% crystal violet for 20 min at room temperature. After rinsing three times with phosphate buffer solution (PBS), cells remaining on the upper surface of the membrane were wiped off with a cotton swab. Images were captured using an inverted microscope, and migratory and invasive cells were counted in representative microscopic fields.

Flow cytometry

Apoptosis was determined using the Annexin V-FITC/PI Cell Apoptosis Detection Kit (TransGen), according to the manufacturer's instructions. Following the respective treatment, cells were trypsinized and stained with Annexin V and PI. Flow cytometry was then utilized to examine the cells, and the data obtained were analyzed using FlowJo V10 software (FlowJo LLC, USA).

Nuclear and cytoplasmic protein extraction

The isolation of nuclear and cytoplasmic fractions was carried out using a Nuclear and Cytoplasmic Protein Extraction Kit (Beyotime), according to the manufacturer's instructions. To confirm the success of the extraction, western blotting was conducted. GAPDH served as a control for cytoplasmic extracts, while histone H3 was employed as a control for nuclear extracts.

Western blotting

The cells were washed with PBS and lysed using RIPA lysis buffer containing protease and phosphatase inhibitors to collect the whole-cell extracts. Protein concentration was determined using a Pierce BCA kit (Thermo Fisher Scientific) following the manufacturer's instructions. Subsequently, cell lysates were separated on 10% polyacrylamide gels and transferred onto polyvinylidene fluoride (PVDF) membranes. After blocking the membranes with 5% bovine serum albumin (BSA) in Tris-buffered saline-Tween 20 (TBST) buffer for 1 h at room temperature, they were incubated overnight at 4°C with primary antibodies. Following washing with TBST buffer, the membranes were subjected to incubation with horseradish peroxidase-conjugated secondary antibodies at room temperature for 1 h. Detection was then performed using HRP Substrate Luminol Reagent (Minipore) with the Tanon analysis system.

Immunohistochemistry

IHC staining was performed on paraffin-embedded sections. The sections were initially dewaxed and hydrated, followed by heating in 10 mM sodium citrate buffer (pH 6.0) for antigen retrieval and blocked with 3% hydrogen peroxide. The primary antibodies against NUAK2 (1:200, Abcam), Ki-67 (1:200, Abcam), SMAD2 (1:500, Proteintech), and SMAD3 (1:500, Proteintech) were applied overnight at 4°C. The antigen–antibody reactions were developed using the REAL EnVision Detection Kit (HRP-linked, Dako). Representative images were captured using an Olympus light microscopy.

Co-immunoprecipitation assay

Pierce Protein A/G Magnetic Beads were used for co-immunoprecipitation assay. The cells were washed with PBS and lysed using RIPA lysis buffer containing protease to collect the proteins. The magnetic beads were resuspended and washed twice. Antibody (Ab) mixtures or anti-rabbit IgG were added to the Protein A/G Magnetic Beads as previously described. After rotating for 4 h at 4°C, the Protein A/G Magnetic Beads-Ab complex was washed and collected for binding with the protein sample containing the antigen (Ag) at 4°C overnight. On the following day, the Ab–Ag complex was collected using an elution buffer. Subsequently, western blotting was performed to confirm these results.

Chromatin immunoprecipitation (CHIP)

ChIP was performed using the BeyoChIP Enzymatic ChIP Assay Kit (Beyotime) according to the manufacturer's instructions. An anti-p65 antibody (Proteintech) was employed to immunoprecipitate proteins from cell lysates with A/G Magnetic Beads conjugated to the anti-p65 antibody. Subsequently, qPCR was performed to analyze the enrichment of NUAK2. The primers used for ChIP-qPCR are detailed in Table S1.

Dual-luciferase reporter assay

The plasmids with different mutant forms of the NUAK2 promoter region and wild-type (WT) form of the NUAK2 promoter region were constructed. For the luciferase assay, pancreatic cancer cells were plated in 12-well plates and co-transfected with a dual-luciferase reporter and p65 overexpression plasmid by Lipofectamine 3000 (Invitrogen). Luciferase activity was detected using the Dual Luciferase Reporter Gene Assay Kit (Yeasen) according to the manufacturer's instructions. The relative luciferase activity was measured and normalized to the activity of Renilla luciferase.

Animal experiments

The *in vivo* experiments were approved by the Committee on Ethics of Beijing Vitalstar Biotechnology Company. Mice were randomly divided into two groups: NUAK2 knockdown (Sh-NUAK2) and control groups (Sh-NC), each consisting of seven mice. Stable cell lines transfected with the Sh-NUAK2 virus and corresponding Sh-NC virus were constructed. Cell suspensions containing 5×10^6 stable cells were subcutaneously inoculated into the back of each mouse. The tumor volume was measured once a week for 4 weeks, and the formula (width$^2\times$length)/2 was used to calculate the tumor volume. After four weeks, the mice were sacrificed and the tumors were collected, measured, and weighed.

QUANTIFICATION AND STATISTICAL ANALYSIS

The data were presented as the mean values with standard deviations. All statistical analyses were performed using GraphPad Prism version 9.0 (GraphPad Software, USA). Student's *t* test was employed for statistical comparisons to assess the differences between the test groups. GraphPad Prism software was used for data visualization. A p-value less than 0.05 was considered statistically significant (*$p < 0.05$, **$p < 0.01$, ***$p < 0.001$).